J|A|C|S
ARTICLES
Published on Web 02/25/2006

Lanthanide Labeling Offers Fast NMR Approach to 3D Structure Determinations of Protein−Protein Complexes

Guido Pintacuda,[†,‡] Ah Young Park,[†] Max A. Keniry,[†] Nicholas E. Dixon,[†] and Gottfried Otting*[,†]

Contribution from the Research School of Chemistry, Australian National University, Canberra ACT 0200, Australia, and Laboratoire de Chimie, Ecole Normale Superieure de Lyon, 46 Allee d'Italie, 69364 Lyon, France

Received October 13, 2005; E-mail: gottfried.otting@anu.edu.au

Abstract: A novel nuclear magnetic resonance (NMR) strategy based on labeling with lanthanides achieves rapid determinations of accurate three-dimensional (3D) structures of protein−protein complexes. The method employs pseudocontact shifts (PCS) induced by a site-specifically bound lanthanide ion to anchor the coordinate system of the magnetic susceptibility tensor in the molecular frames of the two molecules. Simple superposition of the tensors detected in the two protein molecules brings them together in a 3D model of the protein−protein complex. The method is demonstrated with the 30 kDa complex between two subunits of *Escherichia coli* polymerase III, comprising the N-terminal domain of the exonuclease subunit ϵ and the subunit θ. The 3D structures of the individual molecules were docked based on a limited number of PCS observed in 2D ^{15}N-heteronuclear single quantum coherence spectra. Degeneracies in the mutual orientation of the protein structures were resolved by the use of two different lanthanide ions, Dy^{3+} and Er^{3+}.

Protein−protein interactions are most frequently probed by site-directed mutagenesis experiments that provide little insight into the structural details of the interaction. On the other hand, the determination of the three-dimensional (3D)[1] structure of a protein−protein complex by X-ray crystallography or nuclear magnetic resonance (NMR) spectroscopy usually amounts to the equivalent of a full structure determination of a protein of larger size. Here we present an alternative NMR strategy that competes with site-directed mutagenesis in speed, yet provides an accurate 3D representation of the protein−protein complex. The requisite NMR spectra are quick to record and can be evaluated automatically.

Our method is based on the coordinate frame associated with the anisotropic magnetic susceptibility (χ) tensors[2] of certain paramagnetic metal ions. These offer a rich source of long-range structural information that can readily be read from the ^{1}H NMR spectrum, including strongly enhanced relaxation rates of the ^{1}H spins close to the metal ion and changes in chemical shifts (pseudocontact shifts, PCS) that can be observed up to about 40 Å from the paramagnetic center.[3] PCS depend on the position of the nuclear spins with respect to the $\Delta\chi$ tensor of the paramagnetic metal ion, which describes the anisotropic part of the χ tensor:

$$\Delta\delta^{\mathrm{PCS}} = \frac{1}{12\pi r^3}\left[\Delta\chi_{\mathrm{ax}}(3\cos^2\theta - 1) + \frac{3}{2}\Delta\chi_{\mathrm{rh}}\sin^2\theta\cos 2\varphi\right] \quad (1)$$

where $\Delta\delta^{\mathrm{PCS}}$ denotes the difference in chemical shifts measured between diamagnetic and paramagnetic samples, $\Delta\chi_{\mathrm{ax}}$ and $\Delta\chi_{\mathrm{rh}}$ denote the axial and rhombic components of the $\Delta\chi$ tensor, r is the distance of the metal ion from the nuclear spin, and the angles θ and φ describe the orientation of the $\Delta\chi$ tensor with respect to the protein.[2] For metal ions with a nonaxially symmetric $\Delta\chi$ tensor, the $\Delta\chi$ tensor can thus be defined by a Cartesian coordinate system centered at the metal ion with defined orientations of the x, y, and z axes with respect to the molecule. This principal axes system (PAS) can easily be derived from experimentally observed PCS data by minimizing the difference between observed and back-calculated PCS values.

By anchoring a PAS in the molecular frame and providing long-range distance information, PCS data have previously been shown to be uniquely suited for protein structure refinement[4−7] and for determination of structures of protein−protein[8−10] and

* To whom correspondence should be addressed. Phone: +61-2-61256507. Fax: +61-2-61250750.
† Australian National University.
‡ Ecole Normale Superieure de Lyon.

(1) Abbreviations that were used follow: ϵ186, the N-terminal domain (residues 2−186) of the ϵ subunit of *E. coli* DNA polymerase III; 3D, three-dimensional; HSQC, heteronuclear single quantum coherence; NMR, nuclear magnetic resonance; NOE, nuclear Overhauser effect; PAS, principal axes system; PCS, pseudocontact shifts; rmsd, root-mean-square deviation.

(2) Bertini, L.; Luchinat, C.; Parigi, G. *Prog. Nucl. Magn. Reson. Spectrosc.* **2002**, *40*, 249−273.
(3) Allegrozzi, M.; Bertini, I.; Janik, M. B. L.; Lee, Y. M.; Lin, G. H.; Luchinat, C. *J. Am. Chem. Soc.* **2000**, *122*, 4154−4161.
(4) Banci, L.; Bertini, I.; Gori-Savellini, G.; Romagnoli, A.; Turano, P.; Cremonini, M. A.; Luchinat, C.; Gray, H. B. *Proteins* **1997**, *29*, 68−76.
(5) Banci, L.; Bertini, I.; Cremonini, M. A.; Gori-Savellini, G.; Luchinat, C.; Wüthrich, K.; Güntert, P. *J. Biomol. NMR* **1998**, *12*, 553−557.
(6) Hus, J. C.; Marion, D.; Blackledge, M. *J. Mol. Biol.* **2000**, *298*, 927−936.
(7) Banci, L.; Bertini, I.; Cavallaro, G.; Giachetti, A.; Luchinat, C.; Parigi, G. *J. Biomol. NMR* **2004**, *28*, 249−261.

10.1021/ja057008z CCC: $33.50

DNA−ligand complexes.[11−13] Here we show that PCS data alone, recorded with two different paramagnetic lanthanide ions and combined with prior knowledge of the 3D structures of the individual protein molecules, provide straightforward access to 3D structures of protein−protein complexes obtained by rigid-body docking. Only a minimal data set derived from highly sensitive ^{15}N-HSQC (HSQC = heteronuclear single quantum coherence) spectra is required, and the PAS can be derived fully automatically at the same time as the assignment of the ^{15}N-HSQC cross-peaks.[14]

To develop the method, we used the 30 kDa complex between the θ subunit and the N-terminal domain of the ϵ proof-reading exonuclease subunit, ϵ186, of *Escherichia coli* DNA polymerase III. The structure of ϵ186 had been determined by X-ray crystallography,[15] and the structure of isotope-labeled θ bound to unlabeled ϵ186 had been determined by NMR spectroscopy, but the structure of the ϵ186-θ complex was unknown.[16] The ϵ subunit has a pair of Mn^{2+}/Mg^{2+} ions at the active site that can be replaced by a single lanthanide ion, as in the related domain of DNA polymerase I.[17,18] Lanthanide ions can readily be exchanged in the ϵ186−θ complex. NMR spectra were recorded of the diamagnetic apo complex and in the presence of single equivalents of paramagnetic Dy^{3+}, Er^{3+}, or Ho^{3+} ions.

Experimental Section

Protein Samples. The ϵ186 and θ subunits of DNA polymerase III were purified separately from overproducing strains, and the ϵ186−θ complex was assembled and isolated as described.[19] Minimal media supplemented with $^{15}NH_4Cl$ (or $^{15}NH_4Cl$ and ^{13}C-glucose) were used for the production of the uniformly labeled ^{15}N-θ (or ^{13}C/^{15}N-θ) subunit, while minimal media supplemented with ^{15}N-Leu or ^{15}N-Phe were used to make selectively ^{15}N-labeled samples of ϵ186. A sample of ^{2}H/^{15}N-ϵ186 was prepared from cells grown at 30 °C in 2 L of Luria−Bertani medium until $A_{595} = 0.6$. The cells were harvested, washed with 200 mL of ^{2}H/^{15}N-labeled medium (Silantes, OD2), resuspended in 800 mL of the same medium, and treated for 4 h with 1 mM IPTG. Mass spectrometric analysis revealed two signals in about 2:1 ratio, corresponding to fully ^{2}H/^{15}N-labeled and unlabeled ϵ186, respectively.

Complexes with lanthanide ions were prepared at 0.1 mM protein concentrations in a buffer of 20 mM Tris, 100 mM NaCl and 0.1 mM dithiothreitol at pH 7.2 (NMR buffer) by the addition of 3 equivalents of $LnCl_3$, followed by 4 washes with NMR buffer, using a centrifugal ultrafiltration device, where each wash involved an 8-fold dilution with NMR buffer from 0.5 to 4 mL. For the exchange of one lanthanide ion with another, the apo−protein complex was first regenerated by extensive dialysis against NMR buffer with 1 mM EDTA, followed by dialysis against NMR buffer without EDTA. NMR data were recorded with protein samples at 0.5 mM in NMR buffer.

NMR Measurements. All NMR data were recorded at 25 °C at ^{1}H NMR frequencies of 800 and 600 MHz, using Bruker AV800 and Varian Inova 600 NMR spectrometers, respectively. ^{15}N-HSQC spectra of paramagnetic samples were recorded with insensitive nuclei enhanced by polarization transfer (INEPT) periods of 2.2 ms to minimize magnetization losses by ^{1}H relaxation. For the observation of very broad ^{1}H NMR signals, ^{15}N-HSQC spectra were also recorded without a refocusing INEPT period and without decoupling during the acquisition time. In general, ^{15}N-HSQC spectra were recorded using $t_{1max} = 51$ ms, $t_{2max} = 146$ ms, 23 ppm sweep width in the ^{1}H dimension, and total recording times of 5 and 16 h for diamagnetic and paramagnetic samples, respectively

Intermolecular nuclear Overhauser effects (NOEs) between ^{2}H/^{15}N-ϵ186 and unlabeled θ were recorded with 2D nuclear Overhauser enhancement spectra with $^{15}N(\omega_2)$-half-filter and $^{15}N(\omega_1,\omega_2)$-double-half-filter,[20] using a mixing time of 150 ms and total recording times of 24 and 42 h, respectively.

Resonance Assignments and Determination of the Metal-Ion Position. Paramagnetic samples contained single equivalents of Dy^{3+}, Er^{3+}, or Ho^{3+}. The resonance assignments and determination of $\Delta\chi$ tensor parameters for ϵ186 and θ have been described elsewhere.[14,16] Briefly, diamagnetic and paramagnetic ^{15}N-HSQC cross-peaks observed for selectively ^{15}N-Phe and ^{15}N-Leu-labeled samples of ϵ186 in complex with unlabeled θ were assigned by a comparison of diamagnetic and paramagnetic ^{15}N-HSQC spectra, using the program Platypus[14] with the crystal structure of ϵ186.[15] The metal-ion position was refined from its starting position (the coordinates of one of the two Mn^{2+} ions in the crystal structure of ϵ186) by systematically varying the metal position and minimizing the difference between experimental and back-calculated PCS values.[14]

The backbone amide resonances of uniformly ^{15}N/^{13}C-labeled θ were assigned in the diamagnetic apo complex with unlabeled ϵ186, using a conventional set of triple-resonance 3D NMR spectra. Assignments in its Dy^{3+}-, Er^{3+}-, and Ho^{3+}-loaded forms were obtained by inspection of the ^{15}N-HSQC and HNCO spectra of paramagnetic and diamagnetic samples. The PCS values measured by these experiments formed part of the experimental restraints in the structure calculation of θ[16] by the program Xplor-NIH.[7,21] The structure calculations of θ used, besides a conventional set of distance and dihedral angle restraints, the parameters $\Delta\chi_{ax}$ and $\Delta\chi_{rh}$ of the magnetic susceptibility tensor determined for ϵ186 and yielded the orientation of the $\Delta\chi$ tensor and the position of all three lanthanide ions with respect to the 3D structure of θ.[16]

Docking. PCS-based rigid-body docking was carried out with a newly designed routine programmed in Mathematica (Wolfram Research, Inc.). The program performed the following four steps: (i) The experimental PCS data were fitted to each of the two protein structures to determine the orientation of the PAS of the metal susceptibility tensor with respect to the respective protein coordinates, using as variables the axial and rhombic components of the $\Delta\chi$ tensor, $\Delta\chi_{ax}$ and $\Delta\chi_{rh}$, and the three Euler angles describing the relative orientations of the protein coordinates and the PAS. (In an equivalent manner, the PAS and $\Delta\chi$ parameters determined by Platypus[14] or Xplor-NIH[7,21] could have been used. The program would accept those as input.) As a measure of the uncertainties, 20 PAS were calculated for ϵ186 structures modified by the addition of structural noise to the crystal coordinates (PDB code 1J53),[15] generated by random displacements of the positions of the lanthanide ion and amide protons. The displacements followed a Gaussian distribution function with a standard deviation of 0.2 Å, as described.[14] In the case of θ, structural variation was provided by the 12 conformers representing the NMR structure of ϵ186-bound θ.[16] A PAS was calculated for each conformer of the NMR ensemble. (ii) All NMR conformers were superimposed for minimal root-mean-square deviation (rmsd) between the position of the backbone atoms and the

(8) Ubbink, M.; Ejdebäck, M.; Karlsson, B. G.; Bendall, D. S. *Structure* **1998**, *6*, 323−335.
(9) Nocek, J. M.; Huang, K.; Hoffman, B. M. *Proc. Natl. Acad. Sci. U.S.A.* **2000**, *97*, 2538−2543.
(10) Diaz-Moreno, I.; Diaz-Quintana, A.; De la Rosa, M. A.; Ubbink, M. *J. Biol. Chem.* **2005**, *280*, 18908−18915.
(11) Gochin, M. *J. Biomol. NMR* **1998**, *12*, 243−257.
(12) Tu, K.; Gochin, M. *J. Am. Chem. Soc.* **1999**, *121*, 9276−9285.
(13) Gochin, M. *Structure* **2000**, *8*, 441−452.
(14) Pintacuda, G.; Keniry, M. A.; Huber, T.; Park, A. Y.; Dixon, N. E.; Otting, G. *J. Am. Chem. Soc.* **2004**, *126*, 2963−2970.
(15) Hamdan, S.; Carr, P. D.; Brown, S. E.; Ollis, D. L.; Dixon, N. E. *Structure* **2002**, *10*, 535−546.
(16) Keniry, M. A.; Park, A. Y.; Owen, E. A.; Hamdan, S.; Pintacuda, G.; Otting, G.; Dixon, N. E. *J. Bacteriol.* **2006**, submitted for publication.
(17) Brautigam, C. A.; Aschheim, K.; Steitz, T. A. *Chem. Biol.* **1999**, *6*, 901−908.
(18) Frey, M. W.; Frey, S. T.; Horrocks, W. D., Jr.; Kaboord, B. F.; Benkovic, S. J. *Chem. Biol.* **1996**, *3*, 393−403.
(19) Keniry, M. A.; Berthon, H. A.; Yang, J. Y.; Miles, C. S.; Dixon, N. E. *Protein Sci.* **2000**, *9*, 721−733.
(20) Otting, G.; Wüthrich, K. *Q. Rev. Biophys.* **1990**, *23*, 39−96.
(21) Schwieters, C. D.; Kuszewski, J. J.; Tjandra, N.; Clore, G. M. *J. Magn. Reson.* **2003**, *160*, 65−73.

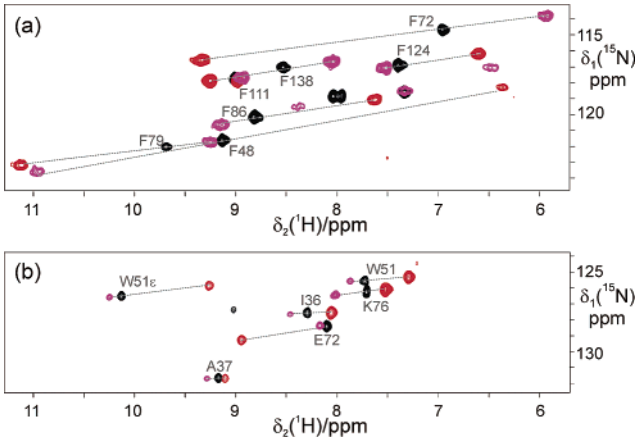

Figure 1. Selected spectral regions of ^{15}N-HSQC spectra recorded of the ϵ186−θ complex with and without paramagnetic lanthanide ions. All spectra were recorded at 25 °C and pH 7.0 using an 800 MHz NMR spectrometer. Superpositions of three spectra are shown for (a) ^{15}N-Phe-labeled ϵ186 in complex with unlabeled θ and (b) uniformly ^{15}N-labeled θ in complex with unlabeled ϵ186. Lines connect cross-peaks of backbone amides recorded without a lanthanide ion (black), with Dy^{3+} (red), and with Er^{3+} (magenta) and are marked with the residue assignments of the cross-peaks.

position of the metal ion. (iii) The ϵ186 conformers were translated for minimum rmsd between the backbone atoms. The 12 θ conformers were translated for complete superposition of the metal-ion positions, including the mean position of the metal ion in the ϵ186 structures. (iv) The bundle of θ conformers was rotated around the metal ion for best superposition between the set of 12 PAS of θ and the set of 20 PAS of ϵ186 (the latter generated by the addition of structural noise), without changing the relative orientations between the different PAS within the individual molecules. This was achieved by searching for a minimum of the generalized angle[22] between the two sets of PAS,

$$\cos\vartheta = \frac{1}{m\times n}\sum_{m,n}\frac{\langle\Delta\chi^{(m)}|\Delta\chi^{(n)}\rangle}{|\Delta\chi^{(m)}||\Delta\chi^{(n)}|} = \frac{1}{m\times n}\sum_{m,n}\frac{\sum_{i,j}\Delta\chi_{ij}^{(m)}\Delta\chi_{ij}^{(n)}}{\sqrt{\sum_{i,j}(\Delta\chi_{ij}^{(m)})^2\sum_{i,j}(\Delta\chi_{ij}^{(n)})^2}} \quad (2)$$

where $\Delta\chi^{(m)}$ and $\Delta\chi^{(n)}$ denote the susceptibility tensors of the Dy^{3+} ion, as determined in each of the m conformers of ϵ186 and n conformers of θ, respectively, and $\Delta\chi_{ij}$ (i, j = x, y, z) are the components of the $\Delta\chi$ tensors in a common reference frame. In addition, the three other (degenerate) minima that were identified arose from 180° rotations of the bundle of θ structures around the x, y, and z axes, respectively, of the PAS of ϵ186. Generalized angles were also calculated to evaluate the fit between the Er^{3+} PAS observed for ϵ186 and θ, following superposition of the Dy^{3+} PAS. In this case, $\Delta\chi^{(m)}$ and $\Delta\chi^{(n)}$ in eq 2 were the susceptibility tensors of the Er^{3+} ions of the m conformers of ϵ186 and the n conformers of θ, respectively.

Results

Measurement of Pseudocontact Shifts. PCS of amide protons were measured from ^{15}N-HSQC spectra of the ϵ186−θ complex, where either ϵ186 had been selectively labeled with ^{15}N-Phe or ^{15}N-Leu[14] or θ had been uniformly ^{15}N labeled (Figure 1).[16]

The assignments of the paramagnetic spectra relied on the similarity of the PCS values of ^{1}H and ^{15}N chemical shifts, arising from the similar positions of the proton and nitrogen atoms of each amide group with respect to the χ tensor. The cross-peaks in the paramagnetic spectra were thus displaced from their diamagnetic counterparts along approximately diagonal lines. In the case of the complex containing uniformly ^{15}N-labeled θ and Dy^{3+}, ambiguities in pairing paramagnetic and diamagnetic peaks were resolved by recording 3D HNCO spectra, where each cross-peak displayed similar PCS in all three dimensions (data not shown). The PCS were measured as the difference in chemical shifts between the diamagnetic spectrum of the apo complex and the paramagnetic spectrum measured with Dy^{3+} and Er^{3+}, respectively.

In most cases, the different $\Delta\chi$ tensor properties of Dy^{3+} and Er^{3+} caused peak shifts in opposite directions that were not simply proportional to each other in magnitude. This suggested that the $\Delta\chi$ tensors of Dy^{3+} and Er^{3+} were not completely aligned. Ambiguities arising from the C_2 symmetries of the $\Delta\chi$ tensor of Dy^{3+} around its x, y, and z axes could thus be resolved by a comparison with the $\Delta\chi$ tensor of Er^{3+}. In contrast, PCS data recorded with Ho^{3+} were almost completely proportional to those measured with Dy^{3+} and, therefore, were not included in the following data analysis.

The orientation of the PAS defined by the $\Delta\chi$ tensor with respect to the molecular frame can be described by three Euler angles. In addition, the $\Delta\chi$ tensor is described by the axial and rhombic components $\Delta\chi_{ax} = \chi_z - (\chi_x + \chi_y)/2$ and $\Delta\chi_{rh} = \chi_x - \chi_y$, respectively. These tensor parameters were derived by minimizing the difference between experimentally measured and back-calculated PCS values, using the coordinates of the X-ray structure of ϵ186, determined in the absence of θ.[15] The optimization included the refinement of the metal-ion position, which shifted by about 0.8 Å from the starting position defined by one of the two Mn^{2+} sites in the crystal structure.[15] These tensors were used to position the structure of θ[16] with respect to the $\Delta\chi$ tensor for best agreement between measured and back-calculated PCS. Figure 2 illustrates the quality of the fits for ϵ186 and θ in the complexes with Dy^{3+} and Er^{3+}. The residual deviations between experimental and back-calculated PCS values were generally much larger than the uncertainty in the PCS measurements (about 0.01 ppm) and, therefore, most likely a result of differences between the crystal structure of ϵ186[15] and the solution structure of ϵ186 in the complex with θ (Figures 2a,b) or a result of inaccuracies in the NMR structure of θ (Figures 2c,d).

Rigid-Body Docking. The PCS generated by the $\Delta\chi$ tensor are readily visualized by plotting the isosurfaces that correspond to the different PCS values. The symmetry of the isosurfaces reflects the symmetry of the $\Delta\chi$ tensor, resulting in near-axial symmetry if the rhombic component $\Delta\chi_{rh}$ is small (Figure 3).

The isosurfaces observed with, for example, Dy^{3+} are the same for both proteins, because they reflect the PCS caused by one and the same Dy^{3+} ion bound to the ϵ186−θ complex. Therefore, superposition of the isosurfaces or, equivalently, the PAS of the $\Delta\chi$ tensor anchored in the molecular frames of ϵ186 and θ, docks both molecules to each other in a single step (Figure 3a). In principle, three further degenerate solutions can be obtained by a rotation around the x, y, and z axis of the

(22) Sass, J.; Cordier, F.; Hoffmann, A.; Rogowski, M.; Cousin, A.; Omichinsky, J. G.; Löwen, H.; Grzesiek, S. *J. Am. Chem. Soc.* **1999**, *121*, 2047−2055.

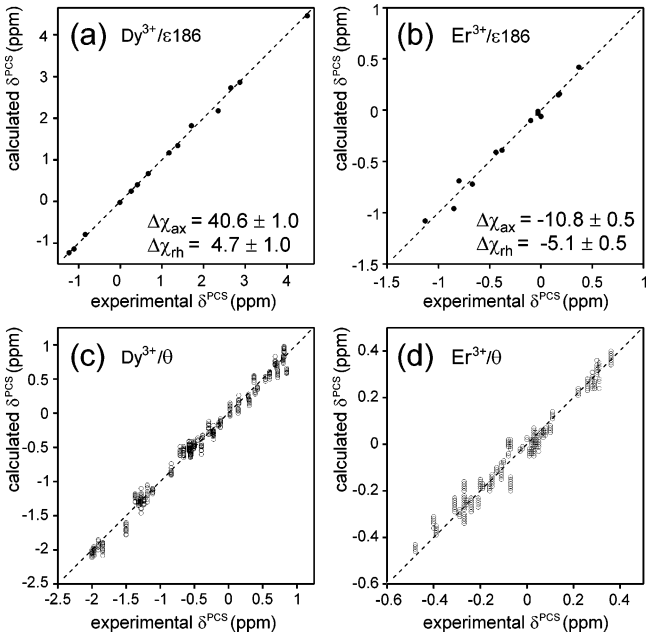

Figure 2. Comparison between experimental and back-calculated PCS of backbone amide protons observed in ϵ186 and θ in the presence of Dy^{3+} and Er^{3+}. The axial and rhombic components of the fitted $\Delta\chi$ tensors are reported in the lower right corner of the correlation plots in SI units (10^{-32} m^3). Note that the $\Delta\chi$ components were erroneously reported 9-fold too small in ref 14. (a) Correlation plot for ^{15}N-Phe-labeled ϵ186 complexed with unlabeled θ and Dy^{3+}. The crystal structure of ϵ186 (PDB code 1J53)[15] was used to back-calculate the PCS. (b) Same as (a), except for the complex with Er^{3+}. (c) Correlation plot for uniformly ^{15}N-labeled θ complexed with unlabeled ϵ186 and Dy^{3+}. The 12 conformers representing the NMR structure of ϵ186-bound θ[16] were used to back-calculate the PCS. (d) Same as (c), except for the complex with Er^{3+}.

PAS.[23] Some of these solutions may be implausible due to severe overlap between the protein molecules or because of no or too few contact points between them.

In the present example, these ambiguities were resolved by the measurement of a second PAS for a second lanthanide ion. Figures 3a,b show that the $\Delta\chi$ tensor of Er^{3+} was smaller than that of Dy^{3+}, of different sign, and with its main axis (the *z* axis) slightly tilted with respect to the main axis of the $\Delta\chi$ tensor of the Dy^{3+} complex. The x and y axes also point in different directions, but their orientations are less well-determined because $\Delta\chi_{rh}$ is smaller than $\Delta\chi_{ax}$.

The differences in the PAS defined by Dy^{3+} and Er^{3+} are most clearly presented by Sanson−Flamsteed projections[24] that mark the penetration points of the x, y, and z principal axes of the $\Delta\chi$ tensors on the surface of a sphere (Figures 3c−h). This representation shows that the orientation of the *z* axis is much less sensitive with regard to small, random structural variations introduced in the crystal structure of ϵ186[15] (angular variation less than ±2° from the mean *z* axis orientation) than the orientations of the x and y axes (angular variation up to about ±20°; Figure 3d). Similarly, the structural variation presented by different conformers of the NMR structure of θ[16] caused larger uncertainties in the orientations of the x and y axes than in the orientation of the *z* axis (Figures 3e−h). They were overall larger for θ than for ϵ186, because the X-ray structure of ϵ186 fits the observed PCS values better than the NMR structure of θ (Figure 2). Importantly, however, the orientations of the three axes of the $\Delta\chi$ tensors of Dy^{3+} and Er^{3+} always appeared in nonoverlapping groups, showing that the noncollinearity between the two tensors was significant.

The agreement between the Sanson−Flamsteed plot of θ and the Sanson−Flamsteed plot of ϵ186 provides a measure of agreement between the PAS of Dy^{3+} and the PAS of Er^{3+} determined for the two proteins. An initial superposition of the Dy^{3+}PAS of θ on the Dy^{3+}PAS of ϵ186 produced a family of structures onto which the Er^{3+}PAS determined for θ were plotted (Figure 3e). Three additional different orientations of θ with respect to ϵ186 were generated by 180° rotations of θ around, respectively, the x (Figure 3f), y (Figure 3g), or *z* axis (Figure 3h) of the average PAS of Dy^{3+} defined by Figure 3e. The PAS of Er^{3+} anchored in the molecular frame of θ were repositioned by these 180° rotations. The agreement of the four different orientations with the experimental data was subsequently assessed by comparison of the Er^{3+} PAS of θ (Figure 3e-h) with the Er^{3+} PAS of ϵ186 (Figure 3d). The best agreement between the Sanson−Flamsteed plot of θ and the Sanson−Flamsteed plot of ϵ186 was obtained for the orientation shown in Figure 3e, resulting in the smallest generalized angle (eq 2) between the two sets of Er^{3+} PAS (20.5°). For the orientations of Figures 3f,g, the x and y axes of the $\Delta\chi$ tensor of Er^{3+} were very differently oriented from those found for ϵ186 (Figure 3d). The generalized angles between the two sets of Er^{3+} PAS calculated for these two orientations were 45.2° and 42.8°, respectively. For the orientation of Figure 3h, the *z* axis of the Er^{3+} tensor was invariably on the opposite side of the *z* axis of the Dy^{3+} tensor compared to the situation in ϵ186 (Figure 3d). In this case, the generalized angle between the Er^{3+} PAS was 33.2°. The remaining differences between the appearance of the Sanson−Flamsteed plot of θ and the appearance of the Sanson−Flamsteed plot of ϵ186 (Figures 3d and e) are explained by limitations in the accuracy of the ϵ186 and θ structures.

Structure of the ϵ186−θ Complex. Figure 3i shows the model of the ϵ186−θ complex obtained from the rigid-body docking procedure described above. Uncertainties in the relative positioning of θ with respect to ϵ186 are presented by displaying the results from the docking protocol applied to all 12 NMR conformers of the θ structure for best pairwise agreement with the PAS established for the randomly varied ϵ186 structures, as described above. The uncertainties are far smaller along the z axis of the $\Delta\chi$ tensor (approximately parallel to helix 1 of θ) than in the orthogonal directions (Figures 3d,e).

The overall structure of the complex reveals θ covering a short helix in ϵ186 (helix 2, in red in Figure 3i). Helix 1 of θ (in blue) is approximately parallel to one of the outer strands of the β-sheet in ϵ186 (strand 3, in yellow). The C-terminal part of helix 3 in θ (red) contacts helix 2 in ϵ186. The model suggests the formation of several intermolecular salt bridges between charged amino acid side chains, while avoiding the burial of charged amino acid side chains in the interface. Only Glu 71 in helix 2 of ϵ186 could potentially be buried by θ, although this side chain would be solvent accessible in at least some of the conformations shown in Figure 3i. The model places all helices of θ farther than 15 Å from the paramagnetic center (magenta sphere in Figure 3i). Because paramagnetic relaxation enhancements broadened beyond detection all H^N resonances

(23) Al-Hashimi, H. M.; Valafar, H.; Terrell, M.; Zartler, E. R.; Eidsness, M. K.; Prestegard, J. H. *J. Magn. Reson.* **2000**, *143*, 402−406.
(24) Fischer, M. W.; Losonczi, J. A.; Weaver, J. L.; Prestegard, J. H. *Biochemistry* **1999**, *38*, 9013−9022.

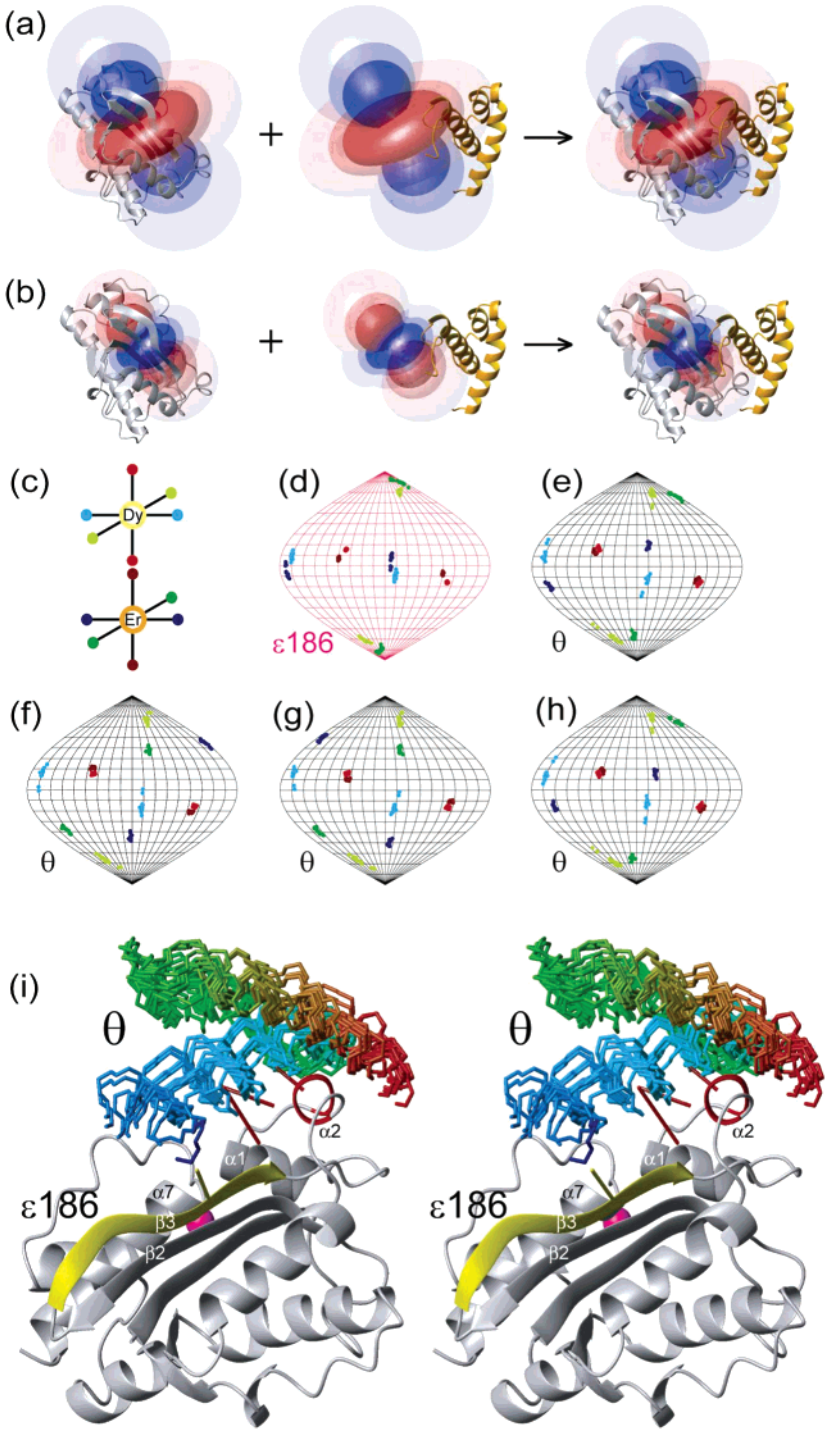

Figure 3. Structure of the $\epsilon 186-\theta$ complex. (a) View of experimentally determined isosurfaces corresponding to PCS of ± 3, ± 1.5, and ± 0.5 ppm. Positive and negative PCS values are indicated by blue and red colors, respectively. The 3D structures of $\epsilon 186$ and θ are represented by gray and yellow ribbons, respectively. Isosurfaces induced by Dy^{3+} are shown plotted on $\epsilon 186$, θ, and the $\epsilon 186-\theta$ complex. (b) Same as (a), except for isosurfaces induced by Er^{3+}. (c) Color coding used for the principal axes of the $\Delta\chi$ tensors from Dy^{3+} and Er^{3+}: *z*-axis, red; *y*-axis, green; *x*-axis, blue. Light and dark hues mark the tensor axes from Dy^{3+} and Er^{3+}, respectively. (d) Sanson-Flamsteed projection showing the orientations of the principal axes of the electronic magnetic susceptibility tensor χ of Dy^{3+} and Er^{3+} with respect to $\epsilon 186$ in the $\epsilon 186-\theta$ complex. The tensor orientations were obtained from fitting the PCS values measured for ^{15}N-Leu- and ^{15}N-Phe-labeled $\epsilon 186$ to the crystal structure of $\epsilon 186$.[15] For visualization of the uncertainties, the fits were repeated with 19 structures of $\epsilon 186$ randomly varied by the addition of structural noise and the data plotted for all 20 PAS (see Experimental Section). (e)−(h) Tensor orientations obtained from fitting the PCS values measured for ^{15}N-θ to the individual conformers representing the NMR structure of θ.[16] The family of 12 θ conformers was oriented such that the χ tensor of Dy^{3+} had the same average orientation in the θ conformers as in the randomized $\epsilon 186$ structure. The solutions in (f), (g), and (h) were generated by 180° rotations of the θ conformers around the average x, y, and z axes, respectively, of the χ tensors of Dy^{3+} with respect to the solution shown in (e). The closest agreement of the Er^{3+} tensor axes in θ with those in $\epsilon 186$ is found in (e). The plots were generated with Mathematica (Wolfram Research, Inc.). (i) Stereoview of the experimentally determined structure of the complex between $\epsilon 186$ and θ, as determined by rigid-body docking using only PCS data from amide protons of complexes with Dy^{3+} and Er^{3+}. The backbone of $\epsilon 186$ is shown in ribbons format, and the 12 NMR conformers of θ are colored from blue at the N-terminus to red at the C-terminus. The position of the lanthanide ion is indicated by the magenta sphere, and straight red and yellow lines identify intermolecular NOEs (Table 1). The average pairwise rmsd of the backbone atoms of residues 10−66 of θ is 2.6 Å. The views of (a), (b), and (i) were generated with Molmol.[52]

Table 1. Intermolecular NOEs between ϵ186 and θ

proton group in θ	proton in ϵ186
Ala 6 $C^{\beta}H_3$	His 49 H^N
Leu 20 $C^{\delta}H_3$	Ile 68 H^N
Leu 20 $C^{\delta}H_3$	Ala 69 H^N
Ala 23 $C^{\beta}H_3$	Phe 72 H^N

within a radius of about 15 Å from the Dy^{3+} ion, this result explains the ready observation of virtually all H^N resonances of residues 9−76 of θ as resolved peaks in the ^{15}N-HSQC spectrum of the ϵ186−θ/Dy^{3+} complex.

As expected for rigid-body docking, the model generated steric clashes involving amino acid side chains. Nevertheless, in nearly all of the superimposed structures in Figure 3i, all of the backbone atoms of ϵ186 and θ were separated by more than 3 Å (considering only the structurally well-defined part of θ, comprising residues 10−66[16]). Most of the steric clashes could, therefore, be easily released by conformational adjustments of amino acid side chains.

Agreement with Intermolecular NOEs and Chemical Shift Changes. Independent verification of our model of the ϵ186−θ complex comes from intermolecular NOEs observed in samples prepared with ^{15}N/^{2}H-labeled ϵ186 and unlabeled θ and with ^{15}N-labeled θ and unlabeled ϵ186 (Table 1). They agreed with the PCS-derived structure of Figure 3i. In addition, the NOE between Ala 6 of θ and His 47 of ϵ186 showed that the N-terminal segment of θ binds to the outer strand of the β-sheet in ϵ186 (yellow in Figure 3i). This structural detail could not be derived from the rigid-body docking, because the N-terminal segment of θ was not structurally defined in the NMR structure of θ.[16] (Figure 3i displays the backbone of residues 6−9 for only a single one of the twelve conformers of θ.) Yet, the NOE could readily be accommodated in the structure of Figure 3i.

Significant changes in chemical shifts observed between free ϵ186 and ϵ186 in complex with θ were reported for helices 1 and 2, in the β strands 2 and 3 and at the N-terminus of helix 7 (Figure 3i).[25] In our structure of the complex, θ contacts helix 2 and strand 3, suggesting that the chemical shift changes in helices 1 and 7 and strand 2 are due to indirect effects.

For θ, the chemical shifts of the N-terminal segment, the entire helix 1 (blue), and the C-terminal part of helix 3 (red) are strongly affected upon binding to ϵ186, while helix 2 (green) and the N-terminal part of helix 3 are essentially unaffected.[16] These observations are also explained by our structure, where these segments of θ do not contact ϵ186. Finally, the pronounced high-field shifts of the methyl protons of Leu 20 of θ in the complex[16] are explained by ring currents from Tyr 51 or Phe 72 of ϵ186.

Discussion

The present approach for the structure determination of protein−protein complexes is fundamentally different from methods using spin labels[26−29] or paramagnetic metal ions (e.g., Cu^{2+}, Mn^{2+}, or Gd^{3+}) that only yield distance-dependent paramagnetic relaxation enhancements and no changes in chemical shifts.[30−34] PCS are much richer in information content, providing exceptionally fast access to 3D structures of protein−protein complexes.

Docking Based on PCS versus other NMR Data. In principle, the knowledge of the 3D structure of the protein components and a minimum of eight PCS values allows the determination of the five variables defining the $\Delta\chi$ tensor of the lanthanide ion ($\Delta\chi_{ax}$, $\Delta\chi_{rh}$, and three Euler angles) and the adjustment of the position of the lanthanide ion with respect to the protein. Additional PCS values result in an over-determined system, greatly improving the accuracy of the $\Delta\chi$ tensor determination in critical situations, as in the case of θ, where the metal ion is located far from the ligand molecule, and all restraints project to one side of the metal ion. ^{15}N-HSQC spectra contain sufficient data for accurate determinations of $\Delta\chi$ tensors, and data recorded with different paramagnetic lanthanide ions contain unambiguous information about the relative orientation of two proteins by providing different $\Delta\chi$ tensors with differently oriented PAS.

The $\Delta\chi$ tensor can be determined automatically with the program Platypus,[14] using selectively ^{15}N-labeled protein samples with and without paramagnetic lanthanide ion, without any prior knowledge of the resonance assignments of either the diamagnetic or the paramagnetic protein. The PCS values of ϵ186 used in the present study had been determined in this manner, using the crystal structure of ϵ186 (without bound θ)[15] and ^{15}N-HSQC spectra of ^{15}N-Leu- and ^{15}N-Phe-labeled ϵ186 samples in complex with unlabeled θ.[14] In the case of θ, PCS values were measured of uniformly ^{15}N- and ^{15}N/^{13}C-labeled samples, because such samples had already been prepared for structure determination by NMR spectroscopy,[16] and no crystal structure was available. Notably, for proteins of known 3D structure and known backbone resonance assignments in the diamagnetic state, the $\Delta\chi$ tensor can also automatically be determined from uniformly ^{15}N-labeled samples.[35] These automation options enhance the speed of our strategy.

The chemical similarity between different lanthanide ions ensures that they bind to the same site with conserved coordination geometry. Combined with their different paramagnetic properties covering different distance ranges,[3] this makes lanthanide ions uniquely suited for this approach.

The method described here is capable of delivering structural information on protein−protein complexes with outstanding accuracy and speed. Most importantly, PCS data simultaneously define the orientation of the protein molecules with respect to the susceptibility tensor *and* their distance from the paramagnetic center. For comparison, docking procedures based on residual dipolar couplings (RDC)[36−38] alone cannot resolve translational

(25) DeRose, E. F.; Darden, T.; Harvey, S.; Gabel, S.; Perrino, F. W.; Schaaper, R. M.; London, R. E. *Biochemistry* **2003**, *42*, 3635−3644.
(26) Barbieri, R.; Bertini, I.; Cavallaro, G.; Lee, Y. M.; Luchinat, C.; Rosato, A. *J. Am. Chem. Soc.* **2002**, *124*, 5581−5587.
(27) Bertini, I.; Luchinat, C.; Parigi, G. *Solution NMR of Paramagnetic Molecules: Applications to Metallobiomolecules and Models*; Elsevier: Amsterdam, 2001.
(28) Ghose, R.; Prestegard, J. H. *J. Magn. Reson.* **1997**, *128*, 138−143.
(29) Boisbouvier, J.; Gans, P.; Blackledge, M.; Brutscher, B.; Marion, D. *J. Am. Chem. Soc.* **1999**, *121*, 7700−7701.
(30) Pintacuda, G.; Moshref, A.; Leonchiks, A.; Sharipo, A.; Otting, G. *J. Biomol. NMR* **2004**, *29*, 351−361.
(31) Donaldson, L. W.; Skrynnikov, N. R.; Choy, W. Y.; Muhandiram, D. R.; Sarkar, B.; Forman-Kay, J. D.; Kay, L. E. *J. Am. Chem. Soc.* **2001**, *123*, 9843−9847.
(32) Mal, T. K.; Ikura, M.; Kay, L. E. *J. Am. Chem. Soc.* **2002**, *124*, 14002−14003.
(33) Iwahara, J.; Anderson, D. E.; Murphy, E. C.; Clore, G. M. *J. Am. Chem. Soc.* **2003**, *125*, 6634−6635.
(34) Iwahara, J.; Schwieters, C. D.; Clore, G. M. *J. Am. Chem. Soc.* **2004**, *126*, 5879−5896.
(35) Schmitz, C.; John, M.; Park, A. Y.; Dixon, N. E.; Pintacuda, G.; Otting, G.; Huber, T. *J. Biomol. NMR* **2006**, in press.
(36) Clore, G. M. *Proc. Natl. Acad. Sci. U.S.A.* **2000**, *97*, 9021−9025.

ambiguities, are much less tolerant with respect to small structural variations (e.g., structural changes as a consequence of complex formation), and cannot be used without prior assignment of the NMR spectrum of the complex. Rigid-body docking based on intermolecular NOEs[20] requires experiments that are far less sensitive than ^{15}N-HSQC spectra, and the assignment of NOE cross-peaks is often difficult.

Proteins without a Natural Metal-Binding Site. The present approach will be applicable to complexes much larger than the 30 kDa ϵ186$-\theta$ complex and appears to be limited mainly by the requirement of a specific lanthanide binding site. This problem can be solved by the use of chemical derivatives of cysteine side chains with suitable lanthanide-binding chelators[30,39−44] or by fusion with a lanthanide-binding peptide.[45,46]

Although the PAS are only slightly tilted between different lanthanides,[46,47] variations of this magnitude have previously been used in RDC measurements to resolve degeneracies by the use of different media that produce differently oriented alignment tensors.[23,48] Chemical modification of cysteine side chains with different lanthanide binding agents will provide access to much more different orientations of $\Delta\chi$ tensors.

Comparison of the ϵ186$-\theta$ Complex with the Structure of Exonuclease I. The principal binding site of θ is far from the catalytic site of ϵ186. Notably, the structure of the nine N-terminal residues of θ has not been defined in the complex with ϵ186.[16] Yet, it is clear that θ cannot access the active site of ϵ186 (although the N-terminal residues of θ may project toward the active site in ϵ186), because ^{15}N-HSQC cross-peaks could be observed for residues 4−9 in the presence of Ho^{3+} and Er^{3+}, which is only possible if the amide protons of these residues are located at least 14 Å from the metal ion to escape excessive paramagnetic line broadening. In conclusion, the modest stimulation of activity of ϵ186 by θ[49] must be a result of indirect effects, possibly by changing the mobility of the ϵ186 molecule,[25,50] or by long-range (electrostatic) effects on binding of ϵ to the single- or double-stranded regions of the primer-template DNA substrate.[16] Interestingly, exonuclease I is a close structural relative of ϵ186[15] that contains an additional helical C-terminal domain (residues 360−477) that caps the core structure of the exonuclease domain at a position that, at the corresponding site of ϵ186, would partially overlap with the binding site of θ.[51] However, none of the helices in the C-terminal domain of exonuclease I superimpose with any of the helices of θ, and the binding site overlap is largely confined to the short loop region between helix 1 and helix 2 of ϵ186. The structural homology is, thus, too low to comment on specific functional similarities between the C-terminal domain of exonuclease I and θ beyond roles in stabilizing the catalytic exonuclease domain. Notably, the C-terminal domain of exonuclease I is also at least 10 Å from the metal ion(s) at the active site. For further functional characterization, we have commenced studies of the interaction of the ϵ186$-\theta$ complex with DNA model compounds.

Acknowledgment. We thank Dr. Michael John for checking PCS and the intermolecular NOEs between ϵ186 and θ with 3D NMR spectra and Drs. E. F. DeRose and R. E. London for making the chemical shift assignments of apo-ϵ186 in complex with θ and their structure of uncomplexed θ in mixed solvent[53] available prior to publication. Financial support from the Australian Research Council for a Federation Fellowship for G.O., the present project, and the 800-MHz NMR spectrometer at ANU is gratefully acknowledged.

JA057008Z

(37) Dosset, P.; Hus, J. C.; Marion, D.; Blackledge, M. *J. Biomol. NMR* **2001**, *20*, 223−231.
(38) Clore, G. M.; Schwieters, C. D. *J. Am. Chem. Soc.* **2003**, *125*, 2902−2912.
(39) Dvoretsky, A.; Gaponenko, V.; Rosevear, P. R. *FEBS Lett.* **2002**, *528*, 189−192.
(40) Gaponenko, V.; Altieri, A. S.; Li, J.; Byrd, R. A. *J. Biomol. NMR* **2002**, *24*, 143−148.
(41) Gaponenko, V.; Sarma, S. P.; Altieri, A. S.; Horita, D. A.; Li, J.; Byrd, R. A. *J. Biomol. NMR* **2004**, *28*, 205−212.
(42) Ikegami, T.; Verdier, L.; Sakhaii, P.; Grimme, S.; Pescatore, B.; Saxena, K.; Fiebig, K. M.; Griesinger, C. *J. Biomol. NMR* **2004**, *29*, 339−349.
(43) Prudêncio, M.; Rohovec, J.; Peters, J. A.; Tocheva, E.; Boulanger, M. J.; Murphy, M. E.; Hupkes, H. J.; Kosters, W.; Impagliazzo, A.; Ubbink, M. *Chem.-Eur. J.* **2004**, *10*, 3252−3260.
(44) Leonov, A.; Voigt, B.; Rodriguez-Castaneda, F.; Sakhaii, P.; Griesinger, C. *Chem.-Eur. J.* **2005**, *11*, 3342−3348.
(45) Ma, C.; Opella, S. J. *J. Magn. Reson.* **2000**, *146*, 381−384.
(46) Wöhnert, J.; Franz, K. J.; Nitz, M.; Imperiali, B.; Schwalbe, H. *J. Am. Chem. Soc.* **2003**, *125*, 13338−13339.
(47) Bertini, I.; Janik, M. B. L.; Lee, Y. M.; Luchinat, C.; Rosato, A. *J. Am. Chem. Soc.* **2001**, *123*, 4181−4188.
(48) Ramirez, B. E.; Bax, A. *J. Am. Chem. Soc.* **1998**, *120*, 9106−9107.
(49) Studwell-Vaughan, P. S.; O'Donnell, M. *J. Biol. Chem.* **1993**, *268*, 11785−11791.
(50) Taft-Benz, S. A.; Schaaper, R. M. *J. Bacteriol.* **2004**, *186*, 2774−2780.
(51) Breyer, W. A.; Matthews, B. W. *Nat. Struct. Biol.* **2000**, *7*, 1125−1128.
(52) Koradi, R.; Billeter, M.; Wüthrich, K. *J. Mol. Graphics* **1996**, *14*, 51−55.
(53) Mueller, G. A.; Kirby, T. W.; DeRose, E. F.; Li, D.; Schaaper, R. M.; London, R. E. *J. Bacteriol.* **2005**, *187*, 7081−7089.